J. Membrane Biol. 186, 13–21 (2002)
DOI: 10.1007/s00232-001-0131-0

The Journal of
Membrane
Biology



# The $\beta_1$ Subunit but not the $\beta_2$ Subunit Colocalizes with the Human Heart $Na^+$ Channel (hH1) already within the Endoplasmic Reticulum

**T. Zimmer, C. Biskup, C. Bollensdorff, K. Benndorf**
Friedrich Schiller University Jena, Institute of Physiology II, Teichgraben 8, 07740 Jena, Germany

Recieved: 15 May 2001/Revised: 29 September 2001

**Abstract.** Voltage-dependent $Na^+$ channels are heteromultimers consisting of a pore-forming $\alpha$ subunit and accessory $\beta$ subunits. In order to provide more insight into the trafficking and assembly of the cardiac $Na^+$ channel complex, we investigated the subcellular localization of the $Na^+$ channel $\beta_1$ and $\beta_2$ subunits, both in the absence and presence of the human heart $Na^+$ channel (hH1). We fused spectrally distinct variants of the green fluorescent protein (GFP) to hH1 and to the $\beta_1$ and $\beta_2$ subunit, and expressed the optically labeled $\beta$ subunits separately or in combination with hH1 in HEK293 cells. In contrast to the predominant localization of hH1 channels within the endoplasmic reticulum (ER), both $\beta$ subunits were clearly targeted to the plasma membrane when expressing their cDNAs alone. Upon coexpression of the $\alpha$ subunit, the $\beta_1$ subunit was efficiently retained within the ER and found to be colocalized with hH1. In contrast to this, hH1 and the $\beta_2$ subunit were not colocalized, i.e., they were detected mainly within the ER and the plasma membrane, respectively. These results indicate that hH1 and the $\beta_2$ subunit are transported separately to the plasma membrane whereas the hH1/$\beta_1$ complex occurs already within the ER, which possibly facilitates trafficking of the channel complex to the plasma membrane.

**Key words:** Green fluorescent protein (GFP) — Human heart $Na^+$ channel (hH1) — $Na^+$ channel $\beta$ subunits — $Na^+$ channel trafficking — Subunit assembly

## Introduction

Voltage-gated $Na^+$ channels are plasma membrane proteins that mediate the upstroke of the action potential in electrically excitable cells (Catterall, 1992). In human cardiac myocytes, the predominantly expressed $Na^+$-channel $\alpha$ subunit is encoded by the SCN5A isoform that has been cloned by Gellens et al. (1992) and termed hH1. Its significance for the cardiac action potential is well documented (for review *see* Cohen & Barchi, 1992), whereas the function of the accessory $\beta$ subunits is still a matter of controversy. The $\beta_1$ subunit was clearly detected by *in situ* hybridization (Qu et al., 1995), Northern blotting (Isom et al., 1992; Makita, Bennett & George, 1994), Western blotting (Sutkowski & Catterall, 1990) and immunofluorescence (Malhotra et al., 2001), suggesting that this subunit is highly expressed in the mammalian heart. However, purified $Na^+$-channel preparations from chicken and rat heart contained only the respective $\alpha$ subunit (Lombet & Lazdunski, 1984; Cohen & Levitt, 1993), but neither $\alpha/\beta_1$ nor $\alpha/\beta_2$ channel complexes. Moreover, the $\alpha$ subunit shows all properties typical for cardiac $Na^+$ channels and its function is only marginally modified by the $\beta_1$ subunit. The only effects of the $\beta_1$ subunit on the function of wild-type hH1 channels are (1) a moderate acceleration of the recovery from inactivation and (2) an increase of the peak $Na^+$ current upon heterologous expression in oocytes from *Xenopus laevis* (Nuss et al., 1995; Qu et al., 1995). Single-channel experiments showed that the unitary conductance and the open probability at the peak current were similar in the presence and absence of the $\beta_1$ subunit, indicating that coexpression of the $\beta_1$ subunit leads to an increased number of channels in the plasma membrane (Nuss et al., 1995).

In contrast to the $\beta_1$ subunit, investigations on the expression of the $\beta_2$ subunit in the heart gave conflicting results. Previous biochemical and immunological approaches strongly suggested the absence of this protein from cardiac muscle cells (Cohen & Levitt, 1993; Isom et al., 1995), whereas a recent

*Correspondence to:* T. Zimmer; email: tzim@mti-n.uni-jena.de

immunochemical study indicated localization of the $\beta_2$ subunit at the Z lines of adult cardiomyocytes (Malhotra et al., 2001). Cruz et al. (1999) suggested a function of this subunit for cardiac excitability. These authors observed a PKA-dependent $Ca^{2+}$ permeation through heterologously expressed hH1 channels when either the $\beta_1$ or the $\beta_2$ subunit was coexpressed. However, this slip-mode conductance of hH1 channels was not found when coexpressing respective channel subunits in Chinese hamster ovary (CHO) cells (Nuss & Marban, 1999).

The fact that coexpression of the $\beta_1$ subunit increases the number of functional channels in the plasma membrane of *Xenopus* oocytes suggests that the trafficking of hH1 channels to the plasma membrane is enhanced by an assembly with the $\beta_1$ subunit. Therefore, it would be challenging to investigate whether both subunits are colocalized already within the endoplasmic reticulum (ER) and the Golgi apparatus. Such a colocalization has not been shown so far. In addition to this, it is presently not known whether the β subunits themselves contain structural elements promoting the transport to the plasma membrane or whether the intracellular trafficking of the β subunits depends essentially on the presence of the α subunit. In this context, it should be noted that both β subunits are homologous to cell adhesion molecules (CAM) of the Ig superfamiliy (Isom et al., 1995; Isom & Catterall, 1996) and that their extracellular domains bind extracellular matrix molecules (Srinivasan, Schachner & Catterall, 1998; Xiao et al., 1999). These data suggest that the auxiliary β subunits of $Na^+$ channels function independently of the α subunit as CAMs in the plasma membrane. This hypothesis predicts an efficient trafficking of the β subunits to the plasma membrane also in the absence of the α subunit.

In the present study we fused different variants of the green fluorescent protein (GFP, CFP, YFP) to the three $Na^+$ channel subunits (hH1, $\beta_1$, $\beta_2$). The optically labeled $\beta_1$ and $\beta_2$ subunits ($\beta_1$-GFP and $\beta_2$-GFP) as well as α/β subunit combinations (hH1-YFP/$\beta_1$-CFP and hH1-YFP/$\beta_2$-CFP) were expressed in HEK293 cells and their subcellular localization was investigated by confocal laser-scanning microscopy. We show characteristic differences between the $\beta_1$ and $\beta_2$ subunits with respect to their subcellular localization and their potency to colocalize with hH1 channels in endoplasmic reticulum membranes.

## Materials and Methods

### cDNAs of $Na^+$ Channel Subunits

Plasmids pSP64T-hH1, pNa200 and pSPNaβ coding for hH1 (accession No. M77235, Gellens et al., 1992), for the rat brain IIA $Na^+$ channel (accession No. X61149, Auld et al., 1988) and for the rat $\beta_1$ subunit (accession No. M91808, Isom et al., 1992) were kindly provided by A. L. George (Vanderbilt University), A. L. Goldin (University of California) and W. Stühmer (Max Planck Institute, Göttingen), respectively. The $\beta_2$ subunit (accession No. U37026, Isom et al., 1995) was isolated by RT-PCR from the human brain astrocytoma cell line 1321N1. Total RNA was isolated using the RNeasy Midi Kit from Qiagen (Hilden, Germany) and the reverse transcription reaction was done with an oligo-dT primer and Superscript II™ (Gibco BRL, Karlsruhe, Germany). The full-length cDNA was obtained by PCR using oligonucleotides 5′-TTTTTAGCATCTAACCATTCCTCCCTTGT-3′ and 5′-ACAGGGCAGAGAGTGAGAGGAGACAGGACAC-3′. Finally, the resulting fragment was subcloned into the *Hinc*II site of pUC119 and subjected to sequencing analysis.

### Generation of the GFP Fusion Constructs

The GFP sequences were fused in-frame to the cDNAs of the $Na^+$ channel subunits so that the respective N-terminus of the GFP variant was connected with the C-terminus of each of the membrane-anchored $Na^+$ channel subunits. According to the assumed topology of these $Na^+$ channel subunits in the plasma membrane, the GFP variants were exposed into the cytosol upon heterologous expression. The hH1-GFP cDNA was obtained by subcloning of the hH1 cDNA as a *Hind*III/*Tth*111I fragment into the *Hind*III/*Bam*HI sites of expression vector pEGFP-N2 (Clontech, Heidelberg, Germany). The resulting vector pEGFPN2-hH1 was used to obtain the hH1-YFP cDNA by a PCR-mediated exchange of the respective GFP variant, as described in detail in the accompanying paper. The expected fusion protein consisted of the full-length hH1 and the YFP sequence ($hH1_{(1–2016)}$-$YFP_{(1–239)}$). To obtain vectors pEGFPN2-$\beta_1$ and pEBFPNl-$\beta_1$ coding for $\beta_1$-GFP and $\beta_1$-BFP (*see* below), the coding region of the $\beta_1$ subunit was ligated as a *Hind*III/*Bsp*1407I fragment into the *Hind*III/*Bam*Hl sites of plasmid pEGFP-N2 and into the *Hind*III/*Bsp*1201 sites of pEBFF-Nl (Clontech), respectively.

To create an expression plasmid coding for the $\beta_2$-GFP fusion protein (pEGFPN2-$\beta_2$), the coding region of the $\beta_2$ subunit was ligated as a *Hind*III/*Ehe*I fragment into the *Hind*III/*Sma*I sites of pEGFP-N2. The respective *Bsp*1407I, *Ehe*I, *Bsp*120I and *Bam*HI sites were treated with Klenow enzyme to allow blunt end ligation. The fusion constructs were expected to encode the following protein sequences: $\beta_{1(1–212)}$-IHRPVAT-$GFP_{(1–239)}$ ($\beta_1$-GFP) and $\beta_{2(1–213)}$-GIHRPVAT-$GFP_{(1–239)}$ ($\beta_2$-GFP). Linker regions of pEGFP-N2 are underlined. To express the blue-shifted variant CFP of the green fluorescent protein fused to the C-terminus of the $\beta_1$ ($\beta_1$-CFP) and $\beta_2$ subunit ($\beta_2$-CFP), the GFP variant was exchanged for the CFP coding region in pEBFPNl-$\beta_1$ and in pEGFPN2-$\beta_2$, respectively, by a recombinant PCR step. Vector pECFP-ER (Clontech) was used as a template for the isolation of the CFP sequence. The resulting fusion constructs were expected to encode the following protein sequences: $\beta_{1(1–212)}$-ARDPPVAT-$CFP_{(1–239)}$ ($\beta_1$-CFP) and $\beta_{2(1–213)}$-GIHRPVAT – $CFP_{(1–239)}$ ($\beta_2$-CFP). Linker sequences (underlined) were derived from the cloning vectors pEBFP-Nl or pEGFP-N2, respectively.

### Heterologous Expression in Hek293 Cells

Plasmids were amplified in *E. coli* strain DH5α and purified by the Qiagen Plasmid Midi Kit. HEK293 cells were transfected by a standard calcium phosphate-precipitation method using in total 2 to 5 μg of purified plasmid DNA per transfection (60-mm cell culture dishes). The transfection mixture was removed after an incubation time of 24 h and the cells were seeded onto poly-L-lysine coated glass coverslips and cultured in fresh growth medium for 1–2 days before imaging.

### Laser-Scanning Microscopy

Confocal imaging was performed with a Zeiss LSM 510 (Carl Zeiss, Jena, Germany) in essentially the same way as described in the accompanying paper.

### Heterologous Expression in *Xenopus* Oocytes

Capped cRNAs of hH1, of IIA and of the $\beta_1$ subunit were prepared by *Spe*I, *Not*I and *Eco*RI digestion of plasmids pSP64T-hH1, pNa200 and pSPNaβ, respectively, followed by in vitro transcription reaction with SP6 (hH1, $\beta_1$) or T7 (IIA) polymerase according to standard procedures (Sambrook, Fritsch & Maniatis, 1989). The $\beta_2$ subunit was first subcloned as a *Bam*HI/*Hind*III fragment into the same sites of vector pGEMHEnew (Liman, Tytgat & Hess, 1992). The resulting plasmid was linearized by *Hind*III digestion and capped cRNA was prepared using T7 polymerase. For the preparation of capped cRNA encoding $\beta_1$-GFP and $\beta_2$-GFP, the respective coding regions were isolated as *Hind*III/*Not*I fragments from expression plasmids pEGFPN2-$\beta_1$ and pEGFPN2-$\beta_2$ respectively, and subcloned into the *Hind*III/*Not*I sites of pGEMHEnew. Plasmid linearization and in vitro transcription were done using *Not*I and T7 Polymerase, respectively.

Ovarian lobes were obtained from *Xenopus laevis* under anesthesia (0.4% 3-aminobenzoic acid ethyl ester) and transferred to $Ca^{2+}$-free Barth medium (in mM: 84 NaCl, 1 KCl, 2.4 $NaHCO_3$, 0.82 $MgSO_4$, 7.5 Tris/HCl, pH 7.4). Oocytes in stages V and VI were incubated in $Ca^{2+}$-free Barth medium containing 1.2 mg/ml collagenase (type CLS II, Biochrom KG) for 60 to 90 min. After washing repeatedly with Barth medium (mM: 84 NaCl, 1 KC1, 2.4 $NaHCO_3$, 0.82 $MgSo_4$, 0.33 $Ca(NO_3)_2$, 0.41 $CaCl_2$, 7.5 Tris/HCl, pH 7.4) containing 4 μg/ml cefuroxim (Lilly, Gießen, Germany), 50 units/ml penicillin (Sigma), 50 μg/ml streptomycin (Sigma) and 100 (μg/ml neomycin (Sigma, Deisenhofen, Germany), the oocytes were isolated and defolliculated mechanically. Glass micropipettes were used to inject a cRNA volume per oocyte of about 40 to 60 nl. Concentrations of the different cRNA preparations were assessed by agarose gel electrophoresis using the 0.24–9.5 kb RNA ladder from Gibco BRL. The hH1 and IIA cRNAs were diluted to a final concentration of about 0.01 μg/μl. The different cRNAs encoding the β subunit variants were coinjected at a concentration of about 0.05 μg/μl. Thus, the final molar ratio of hH1 to β subunit variant was approximately 1:40 at the cRNA level. Qu et al. (1995) showed that at this ratio the observed increase in current amplitude saturated in case of hH1:$\beta_1$ coinjection. Injected oocytes were incubated for 3 days at 18°C in Barth medium. Under those conditions the amplitude of $I_{Na}$, measured 3 days after injection at the test potential of −25 mV, was between 0.5 to 2.8 μA (hH1, hH1/$\beta_2$, hH1/$\beta_2$-GFP, IIA), and 1.8 to 7.5 μA (hH1/$\beta_1$, hH1/$\beta_1$-GFP, IIA/$\beta_1$, IIA/$\beta_1$-GFP). The recovery from inactivation was determined from $Na^+$ currents with an amplitude between 1.5 to 3 μA.

### Electrophysiology

Whole-cell $Na^+$ currents were recorded with the two-microelectrode voltage clamp technique using a commercial amplifier (OC725C, Warner Instruments, Hamden, CT). The glass microelectrodes were filled with 3 M KC1. The microelectrode resistance was between 0.2 and 0.5 MΩ. The bath solution contained (in mM): 96 NaCl, 2 KCl, 1.8 $CaCl_2$, 1 $MgCl_2$, 10 Hepes/KOH, pH 7.2. The currents were elicited by test potentials from −80 to 40 mV in 5-mV increments from a holding potential of −120 mV. The pulsing frequency was 0.2 Hz. Recovery from inactivation was determined with a standard protocol (Fig. 1*B*, inset) at a frequency of 0.2 Hz. The time constant of inactivation was determined by fitting a monoexponential function to the sodium current decay which yielded reasonable fits at the test potentials indicated in Fig. 3. Recording and analysis of the data were performed on a PC with the ISO2 software (MFK, Niedernhausen, Germany). The sampling rate was generally 20 kHz.

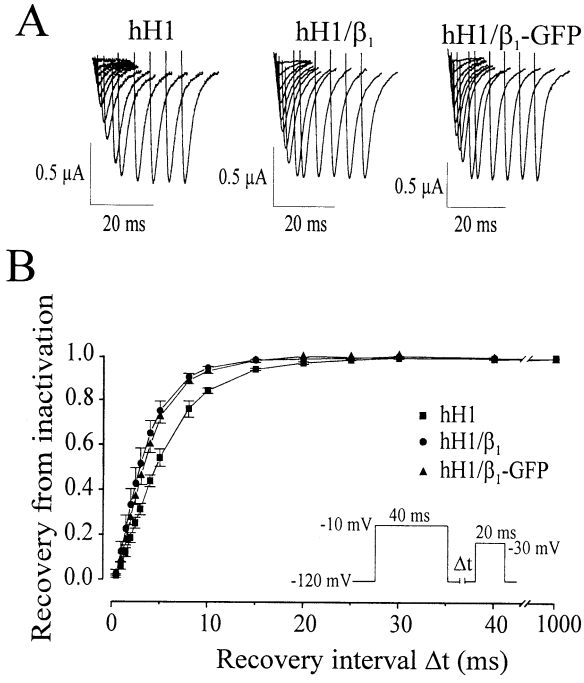


**Fig. 1.** Effect of coexpression of $\beta_1$ and $\beta_1$-GFP on recovery from inactivation of hH1 channels in *Xenopus* oocytes. (*A*) Representative $Na^+$ currents at the test potential of −30 mV. (*B*) Time course of recovery from inactivation. The respective voltage protocol is shown in the inset. The number of individual recordings were: $n = 13$ for hH1, $n = 9$ for hH1/$\beta_1$ and $n = 8$ for hH1/$\beta_1$-GFP. Similar data were obtained using two other batches of oocytes. Bars indicate SEM.

## Results

### Construction and Functional Expression of $\beta_1$-GFP and $\beta_2$-GFP

To study the in vivo distribution of the $\beta_1$ and $\beta_2$ subunits, we fused the green fluorescent protein (GFP) to the cytosolically exposed C-terminus of the $\beta_1$ subunit ($\beta_1$-GFP) and the $\beta_2$ subunit ($\beta_2$-GFP). Before investigating the fluorescence pattern generated by these labeled $\beta_2$ subunits in HEK293 cells, we investigated whether the known functional properties of the $\beta_1$ subunit were unchanged.

The $\beta_1$ subunit increases the cell surface expression of hH1 (Qu et al., 1995) and accelerates the recovery from inactivation (Nuss et al., 1995). Noticeably, both effects were found only in *Xenopus* oocytes, but have not been described yet for a mammalian cell line. This discrepancy could be due

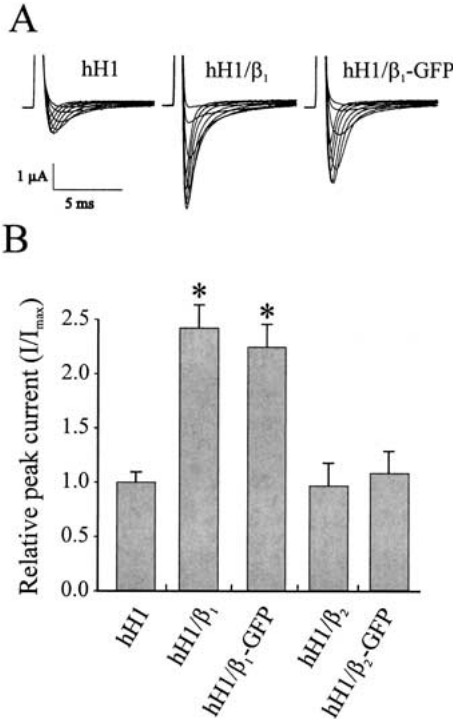


**Fig. 2.** Effect of coexpression of $\beta_1$ and $\beta_1$-GFP on peak current amplitudes in *Xenopus* oocytes. (*A*) Representative families of currents elicited from a holding potential of −120 mV to test potentials of −50, −45, −40, −35, −30, −25, −20, −10 and 0 mV. (*B*) Relative peak current amplitudes. Coexpression of $\beta_1$ and $\beta_2$-GFP significantly increased the number of functional channels in the plasma membrane (*$p < 0.001$). Currents were measured 3 days after injection at the test potential of −25 mV. Measurements were done using 3 different batches of oocytes. Data from a single batch of oocytes were normalized with respect to the mean current of hH1-injected oocytes. Number of measurements were: $n = 36$ for hH1, $n = 31$ for hH1/$\beta_1$, $n = 34$ for hH1/$\beta_1$-GFP, $n = 21$ for hH1/$\beta_2$, and $n = 16$ for hH1/$\beta_2$-GFP. Bars indicate SEM.

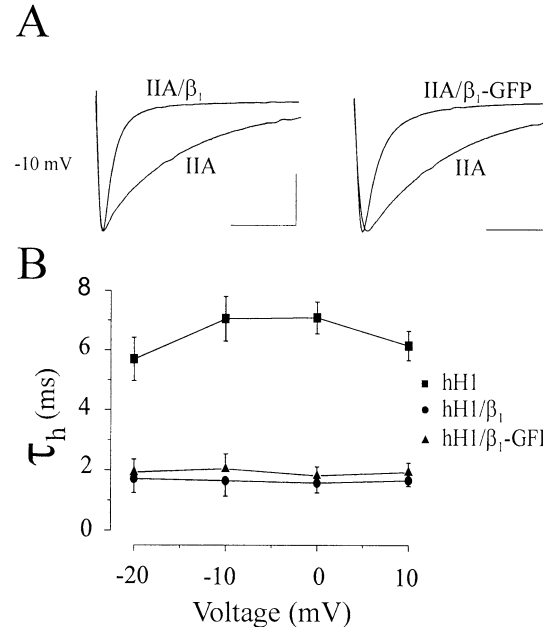


**Fig. 3.** Effect of coexpression of $\beta_1$ and $\beta_1$-GFP on the macroscopic current decay (*A*) and on the time constant of inactivation (*B*) of rat brain IIA $Na^+$ channels. The $Na^+$ currents were elicited by a test pulse to −10 mV, and normalized at the peak current. Calibration bars = 5 msec, 0.6 μA for IIA (*left*), 1 μA for IIA/$\beta_1$, 0.7 μA for IIA (*right*), and 1.2 μA for IIA/$\beta_1$-GFP (*B*). The $Na^+$-current decay was fitted with a monoexponential function. Statistically, $\beta_1$ and $\beta_1$-GFP produced indistinguishable results. The number of recordings were: for $n = 11$ for IIA, $n = 12$ for IIA/$\beta_1$ and $n = 9$ for IIA/$\beta_1$-GFP. Bars indicate SEM.

to the endogenous expression of β subunits in mammalian cells, as observed for $\beta_{1A}$ expression in HEK 293 cells (Moran, Nizzari & Conti, 2000). To analyze the function of $\beta_1$-GFP, we therefore used *Xenopus* oocytes coexpressing hH1 and $\beta_1$ or $\beta_1$-GFP, and measured whole-cell $Na^+$currents by the two-microelectrode voltage clamp technique.

Both $\beta_1$ and $\beta_1$-GFP accelerated the recovery from inactivation of hH1 to a similar extent (Fig. 1). This indicates that the hH1/$\beta_1$ interaction in the plasma membrane was not impaired by the presence of the GFP protein attached to the C-terminus of the $\beta_1$ subunit. At the same time, we detected a significant increase of the peak $Na^+$ current when coexpressing hH1 and the $\beta_1$ subunit (Fig. 2). A similar enlargement of the current amplitude was observed upon coexpression of $\beta_1$-GFP. Interestingly, in contrast to the clear effect of $\beta_1$ and $\beta_1$-GFP, the peak current amplitude was neither enhanced by $\beta_2$ nor $\beta_2$-GFP (Fig. 2*B*). Since previous experiments showed that the $\beta_1$ subunit does not alter single-channel properties of hH1 (Nuss et al., 1995), these findings indicate that only the $\beta_1$ subunit increases the number of functional $Na^+$ channels in the plasma membrane, but not the $\beta_2$ subunit.

To further verify that $\beta_1$-GFP is functionally equivalent to the native protein, we tested the efficacy of this construct to modulate the inactivation kinetics of the rat brain IIA $Na^+$ channel (Auld et al., 1988). As shown in Fig. 3, both $\beta_1$ and $\beta_1$-GFP accelerated the macroscopic current decay significantly, again indicating that the functional integrity of the $\beta_1$ subunit was preserved by linking GFP.

## Subcellular Localization of the $Na^+$-Channel $\beta_1$ and $\beta_2$ Subunits

Expression of $\beta_1$-GFP in HEK293 cells generated a pronounced labeling of the plasma membrane (Fig. 4). We also noticed a fluorescence staining of a fine intracellular membrane network, strongly resembling the smooth ER of eukaryotes. Only occasionally, fluorescent membrane whorls, similar to those observed in cells expressing hH1-GFP, were detected (*not shown*). In contrast to cells expressing hH1-GFP (*see* accompanying paper), we did not detect $\beta_1$-GFP

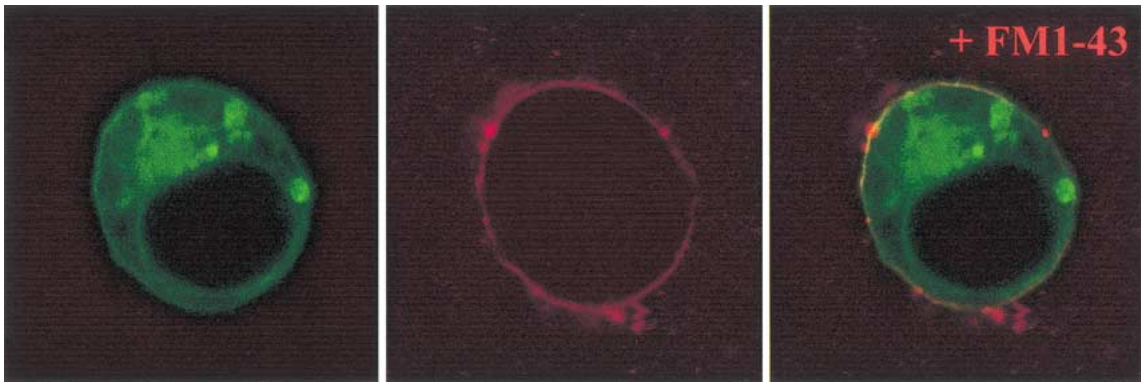


**Fig. 4.** HEK293 cell expressing $\beta_1$-GFP. A dense network of intracellular membranous structures and an intense labeling of the plasma membrane were found by confocal laser-scanning microscopy (*left panel*). A similar fluorescence pattern was observed in all cells investigated, independent of the fluorescence intensity of a transfected cell. Staining of the plasma membrane was conducted using FM1-43 (*middle panel*). Images derived from $\beta_1$-GFP and FM1-43 fluorescence were superimposed to demonstrate localization of $\beta_1$-GFP to the plasma membrane as indicated by the yellow ring (*right panel*).

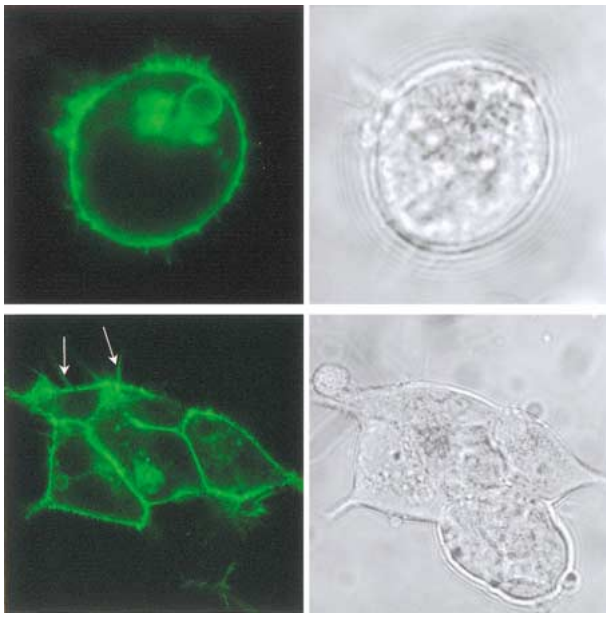

**Fig. 5.** HEK293 cells expressing $\beta_2$-GFP. Fluorescence images observed by confocal laser-scanning microscopy (*left*) and the transmission images (*right*) are shown. The fluorescence pattern of a single HEK293 cell (*upper panel*) and of a transfected cell aggregate (*lower panel*) indicate localization of $\beta_2$-GFP within the plasma membrane and in microvilli (*arrows*). In a few cells, $\beta_2$-GFP containing intracellular membrane whorls were detected (*see* upper panel).

within spherical ER membrane plates surrounding the nucleus.

HEK293 cells expressing the $\beta_2$-GFP fusion protein were characterized by an almost exclusive labeling of the plasma membrane (Fig. 5). Intracellular fluorescent structures appeared as membrane whorls, quite similar to those observed in cells expressing hH1-GFP or $\beta_1$-GFP. Labeling of tubular ER structures or extended membrane plates was not seen. Cells expressing $\beta_2$-GFP produced a unique feature: the fluorescent protein stained filamentous structures (microspikes or microvilli) attached to the cell surface (Fig. 5, *arrows*). These structures were neither detectable in control cells expressing the cytosolic GFP variant (from vector pEGFP-N2) nor in HEK293 cells expressing $\beta_1$-GFP.

These results indicate that the $\beta_1$ and $\beta_2$ subunits are efficiently transported to the plasma membrane in the absence of the α subunit. Differences between the β subunits were found with respect to their intracellular localization and to their ability to form microvilli.

## Coexpression of hH1-YFP and $\beta_1$-CFP or $\beta_2$-CFP

Under the assumption that the $Na^+$ channel α and β subunits assemble to form functional channels, the striking difference between the subcellular distribution of hH1 and both β subunits could be a useful tool to identify the cellular compartment where this assembly may occur. To observe the subcellular localization of different subunits in the same cell, we took advantage of the spectrally different cyan and yellow GFP variants, CFP and YFP, and coexpressed hH1-YFP either with $\beta_1$-CFP or $\beta_2$-CFP.

Coexpression of hH1-YFP and $\beta_1$-CFP generated an indistinguishable fluorescence pattern of the yellow and the cyan fluorescence light (Fig. 6). This result indicates strict colocalization of both subunits. We found predominantly membrane whorls or extended circle-like membranous patterns, which strongly resembled the intensely labeled ER membrane plates of cells expressing hH1-GFP or hH1-YFP alone (*see* accompanying paper). Only a weak fluorescence was observed in the plasma membrane.

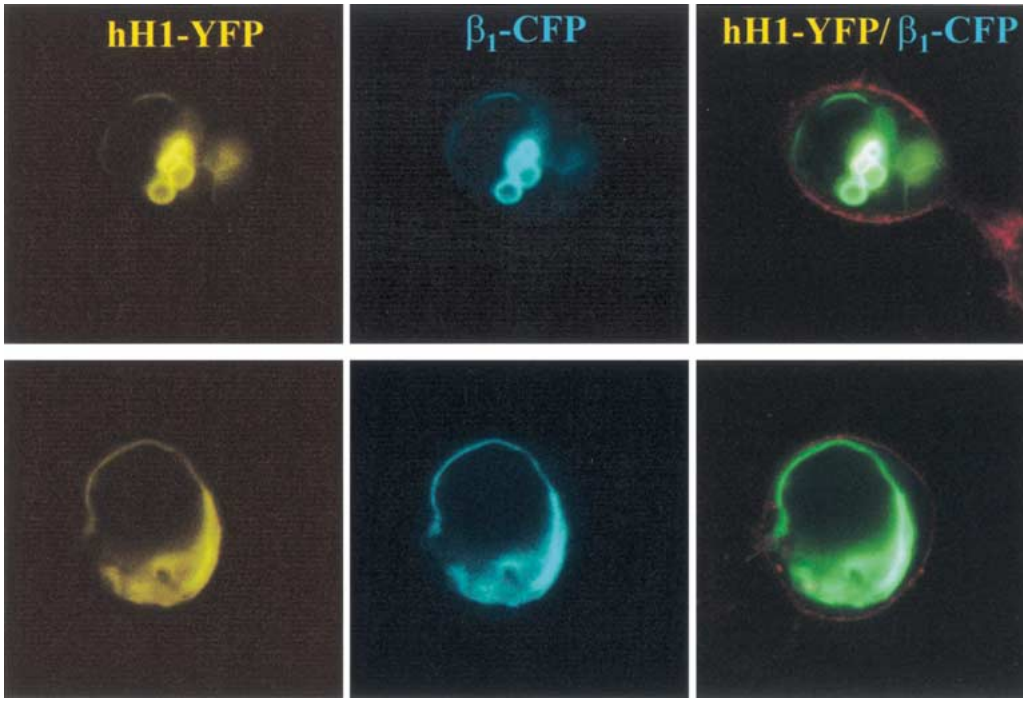


**Fig. 6.** Coexpression of hH1-YFP and $\beta_1$-CFP. The cells were selected first by conventional light microscopy using filter sets that specifically detect either the yellow fluorescence of hH1-YFP (*left*) or the cyan fluorescence of $\beta_1$-CFP (middle) and then observed by laser-scanning microscopy. In the right panels, images derived from hH1-YFP, $\beta_1$-CFP and FM1-43 fluorescence (red) were superimposed to show that the most intensive fluorescence patterns generated by the hH1-YFP and $\beta_1$-CFP molecules were unequivocally localized intracellularly.

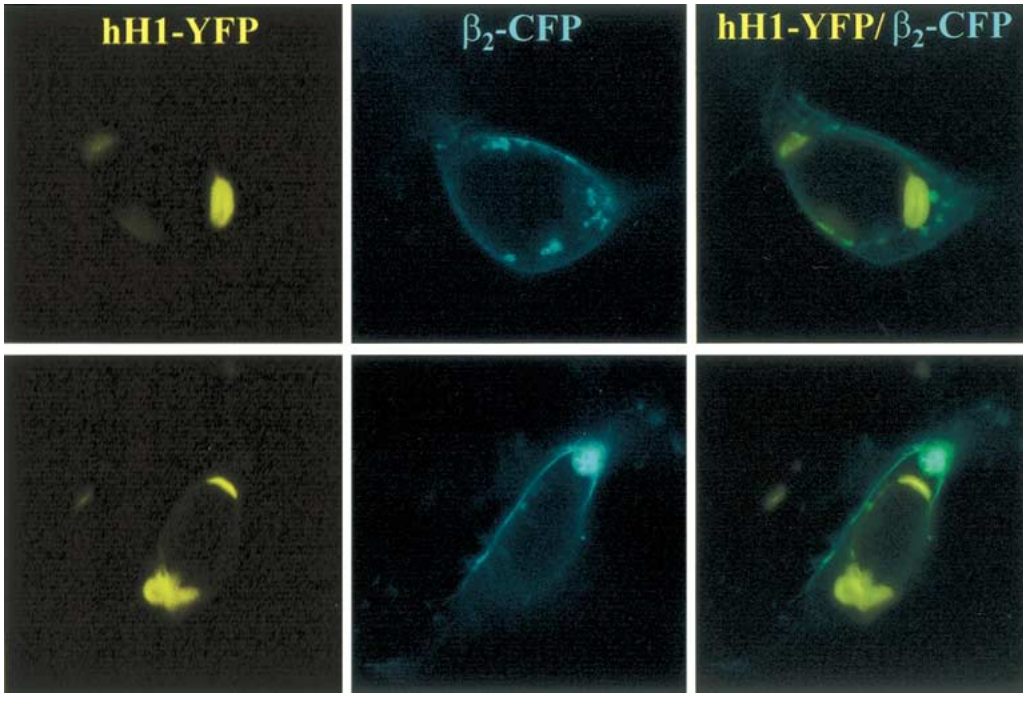


**Fig. 7.** Coexpression of hH1-YFP and $\beta_2$-CFP. In contrast to $\beta_1$-CFP, the subcellular localization of $\beta_2$-CFP (*middle*) was not altered by coexpression of hH1-YFP (*left*). The proteins were not colocalized (*right*).

Thus, the subcellular distribution of the $\beta_1$ subunit was altered by the coexpression of the α subunit (compare localization of the $\beta_1$ subunit in Figs. 4 and 6).

When coexpressing hH1-YFP and $\beta_2$-CFP, the subcellular localization of each of these proteins was unchanged (Fig. 7), compared to their individual expression: hH1-YFP was mainly localized intracellularly within the ER, whereas $\beta_2$-CFP produced a pronounced labeling of the plasma membrane. The intracellular membranes did not exhibit any cyan fluorescence, indicating that, in contrast to $\beta_1$-CFP, $\beta_2$-CFP was not retained by hH1-YFP within the ER.

These data show that the trafficking of the $\beta_1$ subunit to the plasma membrane is altered by the presence of the α subunit. Structural elements underlying this phenomenon are absent or inactive when coexpressing the $\beta_2$ subunit together with hH1 channels.

## Discussion

In the present study we investigated the subcellular localization of the $Na^+$ channel $\beta_1$ and $\beta_2$ subunits in the absence or presence of the α subunit of the human heart $Na^+$ channel (hH1) upon heterologous expression in a mammalian cell line. Our data indicate basic differences between the $\beta_1$ and $\beta_2$ subunit with respect to their subcellular localization and trafficking to the plasma membrane. Moreover, these data provide information about the subcellular compartment, where an assembly of each β subunit with the α subunit may occur.

Expression of $\beta_1$-GFP and $\beta_2$-GFP revealed that, in the absence of hH1, each of the β subunits is predominantly localized within the plasma membrane. In addition to this common feature, transfected HEK293 cells could be distinguished by the different fluorescence pattern generated by the β subunits: $\beta_1$-GFP produced a fine intracellular fluorescent network (Fig. 4), whereas this network was not present upon expression of $\beta_2$-GFP (Fig. 5). This result suggests that only the $\beta_1$ subunit is localized within tubular ER membranes. On the other hand, $\beta_2$-GFP produced stained microvilli (Fig. 5), structures that were not detected upon expression of $\beta_1$-GFP. The additional fluorescent structures that occurred specifically for each of the β subunits were observed in all cells investigated, independent of the overall fluorescence of an individual transfected cell (and, thus, obviously independent of the transfection efficiency). Therefore, we suggest that the morphological differences were not simply due to differences in the expression level. We suppose that these differences reflect intrinsic properties of the individual β subunit.

The most striking difference between the $\beta_1$ and $\beta_2$ subunit was observed in the subcellular distribution upon coexpression with the α subunit. We found an hH1/$\beta_1$ colocalization within the ER in all cotransfected cells, whereas the localization of the $\beta_2$ subunit within the plasma membrane was unaffected. One possible reason for the pronounced retention of the $\beta_1$ subunit is that the hH1-containing ER membranes accommodate the $\beta_1$ subunit nonspecifically. The massive proliferation of the ER might co-induce a retention mechanism for both hH1 and the $\beta_1$ subunit. The second possibility is that the $\beta_1$ subunit is retained specifically within the ER by a molecular interaction with hH1.

The possibility that the $\beta_1$ subunit is nonspecifically retained within hH1-containing membranes is unlikely. One would expect that such a nonspecific retention mechanism inhibits the ER to Golgi transport of other related or unrelated proteins. However, trafficking of both $\beta_2$-CFP (*see* Fig. 7) and also of the Golgi marker YFP-Golgi (*see* Fig. 7 in the accompanying paper) to the plasma membrane and to the Golgi apparatus, respectively, was not impaired by hH1 coexpression. Therefore, we favour the second possibility and suggest that an α/$\beta_1$ subunit assembly occurs already in the ER, similarly as found for many other oligomeric proteins (Hurtley & Helenius, 1989). Moreover, the increased cell-surface expression of hH1 channels upon coexpression of the $\beta_1$ subunit (*see* Fig. 2) has been discussed previously (Qu et al., 1995) as a result of an efficient intracellular interaction of α and $\beta_1$ subunits leading to an enhanced trafficking of the channel complex to the plasma membrane. In our experiments, we also observed an increase in the whole-cell current amplitude upon coexpression of the $\beta_1$ subunit (Fig. 2). The $\beta_2$ subunit, which is not intracellularly colocalized with hH1 (*see* Fig. 7), did not promote cell-surface expression of hH1. Therefore, it seems to be quite reasonable to assume that the strict colocalization of the $Na^+$ channel subunits within the ER is related to an efficient trafficking of the α/$\beta_1$ complex to the plasma membrane.

However, biochemical approaches could not have been previously applied to demonstrate the presence of α/$\beta_1$ complexes in purified membrane fractions of chicken and rat heart (Lombet & Lazdunski, 1984; Cohen & Levitt, 1993). This suggests that the $\beta_1$ subunit dissociates easily from the detergent-solubilized cardiac $Na^+$ channel complex, similarly as shown for rat brain $Na^+$ channels (Messner & Catterall, 1986). Because of this difficulty, our ongoing research is aimed to prove the ER assembly of both $Na^+$-channel subunits in a living cell by a novel fluorescence resonance energy transfer (FRET) technique (Biskup, Zimmer & Benndorf, 2001). If both $Na^+$-channel subunits are associated, the distance between the attached fluorescence probes is supposed to be small enough to allow for sufficient resonance energy transfer from the donor $\beta_1$-CFP to the acceptor hH1-YFP.

When we coexpressed hH1 and the $\beta_2$ subunit we did not find an intracellular colocalization. Structural

elements that determine an hH1-mediated ER-retention mechanism are absent or inactive. Consequently, a large pool of free $\beta_2$ subunits should be present in the plasma membrane. In analogy to our experiments, a large fraction of unbound $\beta_2$ subunits has been found in rat brain neurons (Wollner, Messner & Catterall, 1987). These authors hypothesized an entirely different function of this subunit apart from channel modification. The extracellular domain of the $\beta_2$ subunit is highly homologous to CAMs of the Ig superfamily and recent data provided evidence for the capacity of this subunit to bind extracellular matrix molecules (Srinivasan et al., 1998; Xiao et al., 1999).

The extended microvilli structures that evolved in response to expression of $\beta_2$-GFP (Fig. 5) could be also related to a function as a CAM in promoting cell-cell contacts. Catterall and coworkers investigated the ultrastructure of the *Xenopus* oocyte surface upon expression of the $\beta_2$ subunit, and they found a striking increase in the number and size of microvilli in the plasma membrane associated with an increased cell capacitance (Isom et al., 1995). These data suggest that the enlargement of the cell surface is a specific function of the $\beta_2$ subunit, it occurs independently of the expression system used. The physiological significance of this phenomenon remains, however, to be established.

An interaction of hH1 with the $\beta_2$ subunit in the plasma membrane has been suggested by Cruz et al. (1999) who showed that the accessory $\beta_2$ subunit modulates the conduction properties of hH1 channels in HEK293 cells. Moreover, a recent immunofluorescence study indicated that both the $\beta_1$ and the $\beta_2$ subunit are localized at the Z lines of cardiomyocytes and that at least a portion of rat SCN5A channels is covalently linked to $\beta_2$ (Malhotra et al., 2001). This result suggests the existence of $\alpha/\beta_1/\beta_2$ channel complexes in the plasma membrane of cardiomyocytes. Our data indicate that a corresponding assembly with the $\beta_2$ subunit occurs after the proteins have passed through the Golgi apparatus. This conclusion is consistent with a previous report by Schmidt and Catterall (1986) who found that the assembly of functionally $\alpha/\beta_2$ complexes in rat brain neurons is a late event during the processing of the $Na^+$-channel complex and may occur within the plasma membrane or just before both proteins are inserted into the plasma membrane.

Future studies using chimeric $\beta_1/\beta_2$ subunits are aimed to identify those structural elements in $Na^+$-channel β subunits that are responsible for their subcellular localization and for their colocalization with hH1 in ER membranes. Moreover, it would be challenging to include the newly identified $\beta_{1A}$ (Kazen-Gillespie et al., 2000) and $\beta_3$ (Morgan et al., 2000) subunits in colocalization studies in order to obtain further insight into the biogenesis and function of cardiac $Na^+$-channels.

The authors thank Dr. George and Dr. Kallen for providing the hH1 cDNA, Dr. Goldin for the plasmid pNa200 encoding the rat brain IIA $Na^+$ channel and Dr. Stühmer for providing the rat $\beta_1$ subunit. We also acknowledge the excellent technical assistance of K. Schoknecht, A. Kolchmeier, and S. Bernhardt. This work was supported by a grant from the Deutsche Forschungsgemeinschaft (Be 1250/9-2).

## References

Auld, V.J., Goldin, A.L., Krafte, D.S., Marshall, J., Dunn, J.M., Catterall, W.A., Lester, H.A., Davidson, N., Dunn, R.J. 1988. A rat brain $Na^+$ channel α subunit with novel gating properties. *Neuron* **1:**449–461

Biskup, C., Zimmer, T., Benndorf, K. 2001. Fluorescence lifetime measurements in living cells with a confocal laser-scanning microscope and a streak camera. *Biophys. J.* **80:**656.34

Catterall, W.A. 1992. Cellular and molecular biology of voltage-gated sodium channels. *Physiol. Rev.* **72:**S15–S48

Cohen, S.A., Barchi, R.L. 1992. Cardiac sodium channel structure and function. *Trends Cardiovasc. Med.* **2:**133–140

Cohen, S.A., Levitt, L.K. 1993. Partial characterization of the rHl sodium channel protein from rat heart using subtype-specific antibodies. *Circ. Res.* **73:**735–742

Cruz, J.d.S., Santana, L.F., Frederick, C.A., Isom, L.L., Malhotra, J.D., Mattei, L.N., Kass, R.S., Xia, J., An, R.-H., Lederer, W.J. 1999. Whether "slip-mode conductance" occurs. *Science* **284:**71la (in Technical Comments)

Gellens, M.E., George A.L., Jr., Chen, L., Chahine, M., Horn, R., Barchi, R.L., Kallen, R.G. 1992. Primary structure and functional expression of the human cardiac tetrodotoxin-insensitive voltage-dependent sodium channel. *Proc. Natl. Acad. Sci. USA* **89:**554–558

Hurtley, S.M., Helenius, A. 1989. Protein oligomerization in the endoplasmic reticulum. *Annu. Rev. Cell Biol.* **5:**277–307

Isom, L.L., De Jongh, K.S., Patton, D.E., Reber, B.F.X., Offord, J., Charbonneau, H., Walsh, K., Goldin, A.L., Catterall, W.A. 1992. Primary structure and functional expression of the $\beta_1$ subunit of the rat brain sodium channel. *Science* **256:**839–842

Isom, L.L., Ragsdale, D.S., De Jongh, K.S., Westenbroek, R.E., Reber, B.F.X., Scheuer, T., Catterall, W.A. 1995. Structure and function of the $\beta_2$ subunit of brain sodium channels, a transmembrane glycoprotein with a CAM motif. *Cell* **83:**433–442

Isom, L.L., Catterall, W.A. 1996. $Na^+$ channel subunits and Ig domains. *Nature* **383:**307–308

Kazen-Gillespie, K.A., Ragsdale, D.S., D'Andrea, M.R., Mattei, L.N., Rogers, K.E., Isom, L.L. 2000. Cloning, localization, and functional expression of sodium channel $\beta_{1A}$ subunits. *J. Biol. Chem.* **275:**1079–1088

Liman, E.R., Tytgat, J., Hess, P. 1992. Subunit stoichiometry of a mammalian $K^+$ channel determined by construction of multimeric cDNAs. *Neuron* **9:**861–871

Lombet, A., Lazdunski, M. 1984. Characterization, solubilization, affinity labeling and purification of the cardiac $Na^+$ channel using Tityus toxin gamma. *Eur. J. Biochem.* **141:**651–660

Makita, N., Bennett Jr., P.B., George Jr., A.L. 1994. Voltage-gated $Na^+$ channel $\beta_1$ subunit mRNA expressed in adult human skeletal muscle, heart, and brain is encoded by a single gene. *J. Biol. Chem.* **269:**7571–7578

Malhotra, J.D., Chen, C., Rivolta, I, Abriel, H., Malhotra, R., Mattei, L.N., Brosius, F.C., Kass, R.S., Isom, L.L. 2001. Characterization of sodium channel α- and β-subunits in rat and mouse cardiac myocytes. *Circulation* **103:**1303–1310

Messner, D.J., Catterall, W.A. 1986. The sodium channel from rat brain. Role of the $\beta_1$ and $\beta_2$ subunits in saxitoxin binding. *J. Biol. Chem.* **261:**211–215

Moran, O., Nizzari, M., Conti, F. 2000. Endogenous expression of the $\beta_{1A}$ sodium channel subunit in HEK293 cells. *FEBS Lett.* **473:**132–134

Morgan, K., Stevens, E.B., Shah, B., Cox, P. J., Dixon, A.K., Lee, K., Pinnock, R.D., Hughes, J., Richardson, P.J., Mizuguchi, K., Jackson, A.P. 2000. $\beta_3$: An additional auxiliary subunit of the voltage-sensitive sodium channel that modulates channel gating with distinct kinetics. *Proc. Natl. Acad. Sci. USA* **97:**2308–2313

Nuss, H.B., Chiamvimonvat, N., Perez-Garcia, M.T., Tomaselli, G.F., Marban, E. 1995. Functional association of the $\beta_1$ subunit with human cardiac (hH1) and rat skeletal muscle (μl) sodium channel α subunits expressed in *Xenopus* oocytes. *J. Gen. Physiol.* **106:**1171–1191

Nuss, H.B., Marban, E. 1999. Whether "slip-mode conductance" occurs. *Science* **284:**71la (in Technical Comments)

Qu, Y., Isom, L.L., Westenbroek, R.E., Rogers, J.C., Tanada, T.N., McCormick, K.A., Scheuer, T., Catterall, W.A. 1995. Modulation of cardiac $Na^+$ channel expression in *Xenopus* oocytes by $\beta_1$ subunits. *J. Biol. Chem.* **270:**25696–25701

Sambrook, J., Fritsch, E.F., Maniatis, T. 1989. Molecular Cloning: A Laboratory Manual. Cold Spring Harbor Laboratory Press, Cold Spring Harbor NY.

Schmidt, J.W., Catterall, W.A. 1986. Biosynthesis and processing of the alpha subunit of the voltage-sensitive sodium channel in rat brain neurons. *Cell* **46:**437–445

Srinivasan, J., Schachner, M., Catterall, W.A. 1998. Interaction of voltage-gated sodium channels with the extracellular matrix molecules tenascin-C and tenascin-R. *Proc. Natl. Acad. Sci. USA* **95:**15753–15757

Sutkowski, E.M., Catterall, W.A. 1990. $\beta_1$ subunits of sodium channels. Studies with subunit-specific antibodies. *J. Biol. Chem.* **265:**12393–12399

Wollner, D.A., Messner, D.J., Catterall, W.A. 1987. $\beta_2$ subunits of sodium channels from vertebrate brain. Studies with subunit-specific antibodies. *J. Biol. Chem.* **262:**14709–14715

Xiao, Z.-C., Ragsdale, D.S., Malhotra, J.D., Mattel, L.N., Braun, P.E., Schachner, M., Isom, L.L. 1999. Tenascin-R is a functional modulator of sodium channel β subunits. *J. Biol. Chem.* **274:**26511–26517